

---

# TAIRUS HYDROTHERMAL SYNTHETIC SAPPHIRES DOPED WITH NICKEL AND CHROMIUM

By Victor G. Thomas, Rudolf I. Mashkovtsev, Sergey Z. Smirnov, and Vadim S. Maltsev

*Researchers of the Tairus joint venture have developed the technology for the hydrothermal growth of gem-quality crystals of synthetic sapphire. They have achieved a broad spectrum of attractive colors by varying the concentrations of Ni<sup>2+</sup>, Ni<sup>3+</sup>, and Cr<sup>3+</sup>. Comprehensive testing of 18 faceted synthetic sapphires and 10 synthetic crystals, representing the range of colors, revealed a typical set of internal features that are specific to hydrothermally grown crystals (microscopy), as well as the presence of OH<sup>-</sup> and various carbon-oxygen groups in the sapphire structure (infrared spectroscopy). The reactions of the test samples to ultraviolet radiation and visible light were also found to be useful in distinguishing the Tairus synthetic sapphires from their natural counterparts and other synthetics.*

#### ABOUT THE AUTHORS

*Dr. Thomas is a senior researcher, and Mr. Maltsev is a technological researcher, at Tairus (a joint venture between the Siberian Branch of the Russian Academy of Sciences and Pinky Trading Co. Ltd. of Bangkok, Thailand). Dr. Mashkovtsev is a senior researcher, and Dr. Smirnov is a research scientist, at the Siberian Gemological Center, Novosibirsk*

*Gems & Gemology, Vol. 33, No. 3, pp. 188–202.*

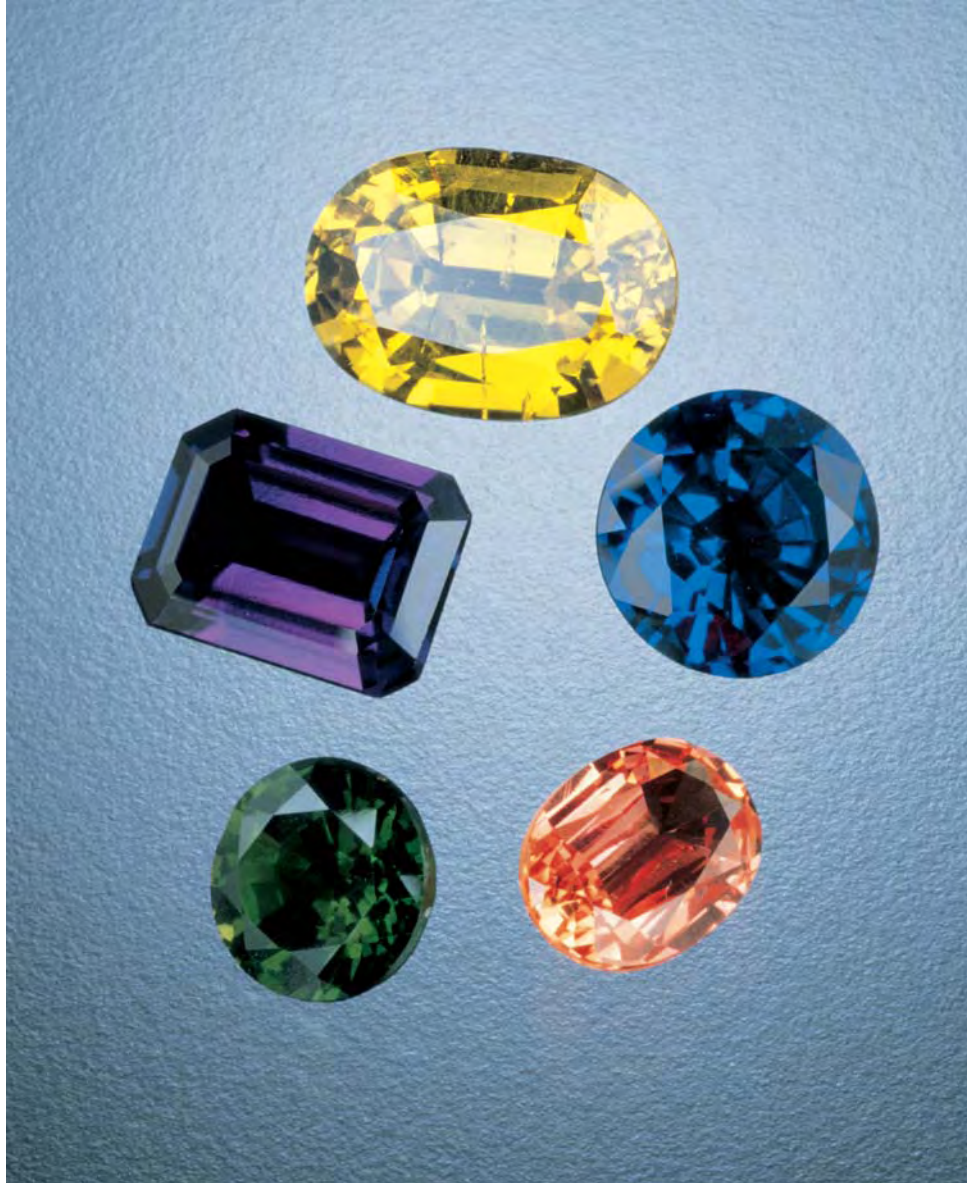
*© 1997 Gemological Institute of America*

The history of hydrothermally grown synthetic corundum began nearly 40 years ago, when Laudise and Ballman (1958) produced the first colorless synthetic sapphire. Their technique, when modified, also can be used to grow rubies (Kuznetsov and Shternberg, 1967). Until recently, however, attempts to grow blue sapphire by the hydrothermal method had failed. This problem is significant because flux-grown and flame-fusion synthetic sapphire crystals typically have uneven color distribution. In blue flame-fusion material, an intense blue hue is usually concentrated in thin outer zones of boules, while most of the bodycolor is much lighter. In blue flux-grown synthetic sapphires, color inhomogeneity is apparent as a sequence of blue and colorless angular growth zones that conform to the crystal shape. Such color inhomogeneity makes cutting difficult and greatly decreases the yield of faceted material.

To address this market gap, the authors investigated the use of hydrothermal growth techniques to produce blue crystals that would be free from the defects of synthetic sapphire grown by other methods. This problem was approached in two ways: (1) by doping hydrothermal synthetic sapphire with iron (Fe<sup>2+</sup>) and titanium (Ti<sup>4+</sup>) ions (as proposed by, for example, Burns, 1981); and (2) by using other doping impurities that could reproduce the blue color of sapphire. Research into the development of a commercial technique by the first approach is still ongoing. However, the second approach has led to success: The use of nickel (Ni<sup>2+</sup>) as a dopant has resulted in crystals of “sky” blue synthetic sapphire, from which thousands of faceted stones as large as 4 ct have been produced by the Tairus joint venture and marketed internationally since 1995.

The next step in the development of this technique was to produce sapphires of different colors by varying the concentrations of Ni<sup>2+</sup>, Ni<sup>3+</sup>, and chromium (Cr<sup>3+</sup>). At this time, the Tairus research group has created the technology

Figure 1. Tairus experts have produced hydrothermal synthetic sapphires in a broad range of colors, as illustrated here. These Tairus synthetic sapphires range from 1.00 to 4.74 ct. Photo © GIA and Tino Hammid.



to grow commercial quantities of sapphires in blue and a wide range of other colors (see, e.g., figure 1). This article presents the results of our research into the growth of hydrothermal synthetic sapphires and their characterization, including the chemistry, gemological properties, and distinctive internal features of these new synthetics.

### GROWTH TECHNIQUES

The autoclave arrangement used to grow Tairus hydrothermal synthetic sapphire is illustrated in figure 2. The growth process is carried out in a hermetically sealed "floating" gold ampoule with a volume of almost 175 ml inside the autoclave, a temperature of 600°C, and a pressure of about 2000 bar. Growth takes place when the initial synthetic colorless sapphire feed is transferred and crystallized onto seeds, via a vertical temperature gradient of 60° to 70°C, through a carbonate solution with a complex composition (the details of which are pro-

prietary). Seed plates oriented parallel to the hexagonal prism  $\{10\bar{1}0\}$  are used to grow cuttable crystals. For research purposes, we also grew two crystals on a spherical seed to investigate the ideal arrangement of the crystal faces. All of the seeds in the samples used for this study were cut from Czochralski-grown colorless synthetic sapphire. The dopant (NiO and, for certain colors,  $\text{Cr}_2\text{O}_3$ ) is introduced via unsealed capsules placed at the bottom of the ampoule. The concentrations of Ni and Cr in the growing crystal are controlled by the diameter of the opening in these capsules.

An oxygen-containing buffer plays a significant role in the sapphire growth process. It is a powdered reagent that is placed at the bottom of each ampoule. This substance governs the valence state of Ni in the solution, so that sapphires with different  $\text{Ni}^{2+}:\text{Ni}^{3+}$  ratios can be grown. Various metals and their oxides (none of which produces any color in the synthetic sapphire) have been used for this

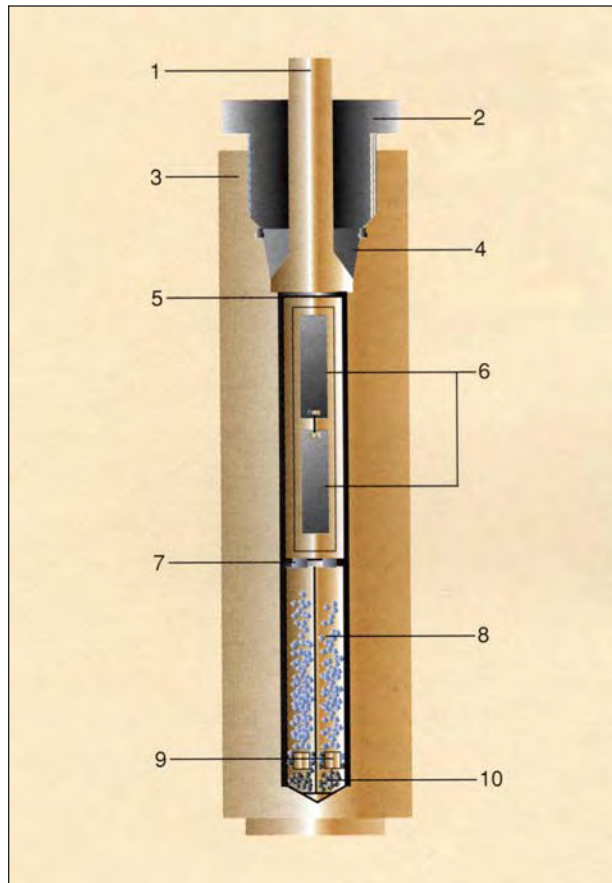


Figure 2. Hydrothermal synthetic sapphires are grown by Tairus scientists in an autoclave that measures 60 cm high and 8 cm in diameter. The components are as follows: (1) lid; (2) push nut; (3) autoclave body; (4) seal ring; (5) gold ampoule; (6) synthetic sapphire seeds; (7) diaphragm; (8) crushed synthetic colorless corundum charge; (9) capsules with Ni/Cr oxides; (10) powdered oxygen-containing buffer. Crystal growth proceeds via dissolution of the corundum charge (8) in a hydrothermal solution in the lower (i.e., hotter) part of the autoclave, followed by convective transfer of the saturated solution to the upper (i.e., cooler) part of the autoclave, where the synthetic sapphire crystallizes on the seeds (6). The autoclave is heated from the bottom and the side in a special furnace.

buffer (e.g., coupled Cu-Cu<sub>2</sub>O, Cu<sub>2</sub>O-CuO, etc. [see table 1]). Synthetic sapphire crystals as large as 7 × 2.5 × 2 cm have been grown in a month, with a growth rate of almost 0.15 mm per day.

### MATERIALS AND METHODS

Two crystals of each color (10 pairs total) were grown under uniform conditions as described above. One crystal in each pair was used to produce faceted gems (from one to five faceted stones, each weighing approximately 1 ct). The other was cut into plates or used whole for crystallographic measurements. Detailed crystallographic measurements were also made on the two greenish blue crystals (each about 0.8 cm across) that were grown on spherical seeds. (These latter crystals were grown both to illustrate the ideal arrangement of crystal faces for corundum produced under the experimental conditions described above, and because it was easier to obtain accurate goniometric measurements on them.) We selected 18 faceted samples (round and oval mixed cuts, weighing about 1 ct each) that ranged from very light pink through orange, yellow, and green to blue (see, e.g., figure 3) for gemological testing. More than 20 polished (on

both sides) plates were used for spectroscopy, inclusion study, and microprobe analysis.

Standard gemological testing was carried out at the Siberian Gemological Center, Novosibirsk. The face-up colors of the 18 faceted synthetic sapphires were determined with a standard daylight-equivalent light source (the fluorescent lamp of a GIA GEM Instruments Gemolite microscope) and an ordinary incandescent lamp. For each faceted sample, the color was compared to standards from the GIA GemSet and described in terms of hue, tone, and saturation. Specific gravity was determined hydrostatically. Refractive indices were measured with a GIA GEM Duplex II refractometer and a filtered, near-monochromatic, sodium-equivalent light source. To examine internal features and polarization behavior, we used a GIA GEM Illuminator polariscope and gemological microscope with various types of illumination.

Detailed observations of inclusions, color zoning, and growth sectors were made on crystal plates of all 10 color varieties with a Zeiss Axiolab polarizing microscope. Some samples were also immersed in methylene iodide for microscopic examination. Appearance in visible light was observed with the incandescent illumination provided by a GIA GEM Instruments spectroscope base, and UV luminescence was observed with the aid of a GIA GEM Instruments ultraviolet cabinet. Samples with weak luminescence were examined in a completely darkened room. Dichroism was determined with a calcite dichroscope and a GIA GEM Instruments FiberLite 150 fiber-optic illuminator.

The arrangement of crystal faces was studied by means of a Zeiss ZRG-3 two-circle goniometer. The

**TABLE 1.** Colors and partial chemistry of the Taurus synthetic sapphires.<sup>a</sup>

Sample	Color	Concentration (wt.%)					TiO <sub>2</sub>
		Cr <sub>2</sub> O <sub>3</sub>	NiO <sup>b</sup>	FeO	MnO	Oxygen buffer	
1	Greenish blue	bdl <sup>c</sup>	0.23	tr	tr	tr	Cu-Cu <sub>2</sub> O
2	Greenish blue	0.15	0.24	tr	tr	tr	Cu-Cu <sub>2</sub> O
3	Greenish blue	0.26	0.34	tr	tr	tr	Cu-Cu <sub>2</sub> O
4	Light reddish purple	0.07	0.04	tr	tr	tr	Cu-Cu <sub>2</sub> O
5	Pink	0.07	bdl	tr	tr	tr	Cu-Cu <sub>2</sub> O
6	"Padparadscha"	0.08	bdl	tr	tr	tr	PbO-Pb <sub>3</sub> O <sub>4</sub>
7	Yellow	tr <sup>d</sup>	tr	tr	tr	tr	PbO-Pb <sub>3</sub> O <sub>4</sub>
8	Light greenish yellow <sup>e</sup>	bdl	tr	tr	tr	tr	Cu-Cu <sub>2</sub> O
9	Green	bdl	0.35	tr	tr	tr	Cu <sub>2</sub> O-CuO
10	Blue-green	bdl	0.23	tr	tr	tr	not controlled
11	Colorless	bdl	bdl	tr	tr	tr	not controlled

<sup>a</sup> Analyses by electron microprobe.<sup>b</sup> Total NiO+Ni<sub>2</sub>O<sub>3</sub>.<sup>c</sup> bdl — below the detection limit = <0.01 wt.%.<sup>d</sup> tr — trace = about 0.02 wt.% for each element.<sup>e</sup> This sample was gamma-irradiated to produce the yellow color (details in Materials and Methods section of text).

compositions (including major and trace elements) of 11 samples representative of the different colors were determined with a Camebax-Micro electron microprobe. We observed visible-range spectra of the 18 faceted stones using a GIA GEM Instruments Prism 1000 spectroscope. In addition, UV-visible spectra were obtained with a Zeiss Specord M40 spectrophotometer, and infrared spectra were measured with Zeiss Specord M80 and SF-20 spectrophotometers, on 1-mm-thick plates. A processor built into the M40 locates the position of absorption band peaks. Color coordinates calculated from the unpolarized absorption spectra were plotted on a CIE chromaticity diagram, to compare color ranges of synthetic sapphires doped with Ni<sup>2+</sup>, Ni<sup>3+</sup>, Cr<sup>3+</sup>, Ni<sup>2+</sup>-Cr<sup>3+</sup>, and Ni<sup>3+</sup>-Cr<sup>3+</sup>. The accuracy of these calculations was checked by a catalogue of colored glass (*Catalogue . . .*, 1967). One hydrothermal synthetic ruby (donated by Alexander Dokukin) and one flame-fusion synthetic ruby were used for com-

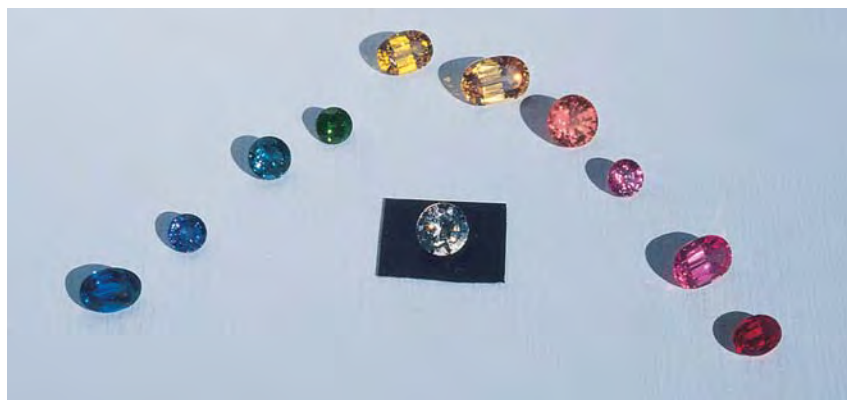
parison in the CIE diagram as examples of corundum doped with Cr<sup>3+</sup> only.

Some of the very light greenish blue sapphires doped with Ni<sup>2+</sup> were gamma irradiated (<sup>60</sup>Co source, dose 0.1–1 Mrad) to convert part of the Ni<sup>2+</sup> to Ni<sup>3+</sup>, which changed the color to yellow. We investigated the ultraviolet and visible spectra on these treated samples.

## RESULTS AND DISCUSSION

**Crystal Morphology.** Crystals grown on flat and spherical seeds are shown in figure 4. These crystals have several sets of major flat faces (i.e., forms) consisting of the hexagonal prism *a* {1120}, dipyrmaid *n* {2243}, and rhombohedron *r* {1011}. These forms are common on natural corundum crystals (Goldschmidt, 1916; Yakubova, 1965). In addition, we observed minor faces of the following forms: rhombohedra *φ* {10 $\bar{1}$ 4} and *d* {10 $\bar{1}$ 2}, as well as rough flat surfaces *θ* {0.1. $\bar{1}$ .11} and *c* {0001} (again, see figure 4).

Figure 3. Although this photo shows the full color range (including colorless and red) of the hydrothermal synthetic corundum produced by Taurus researchers to date (here, 1.11–4.74 ct), the present study focused on those pink, yellow, and green-to-blue synthetic sapphires produced by doping with Ni<sup>2+</sup>, Ni<sup>3+</sup>, and/or Cr<sup>3+</sup>. Photo by Evgeny Krayushin.



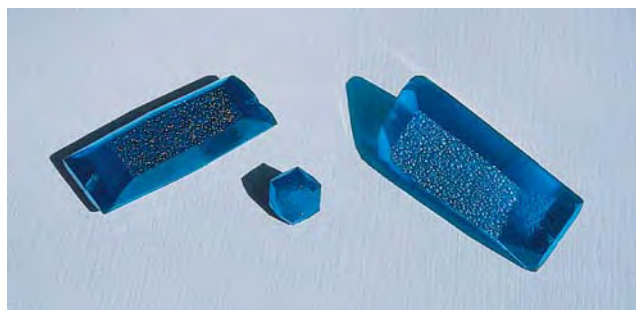
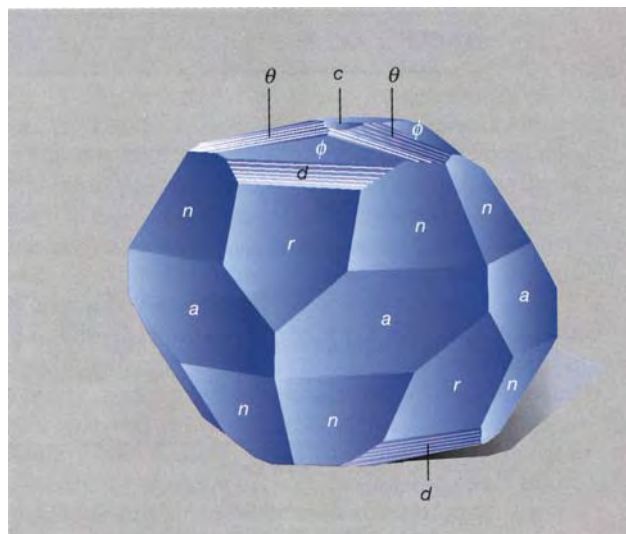


Figure 4. The photo on the left shows two large (5×2 cm) crystals of greenish blue synthetic sapphire that were grown on seed plates, and a small (about 0.8 cm) crystal grown on a spherical seed. (Photo by Evgeny Krayushin.) The line illustration on the right shows the actual crystal faces obtained on a crystal grown on a spherical seed.



With the exception of *c*, these forms are not typical of natural corundum crystals. The Miller indices of the  $\phi$  and  $\theta$  faces were calculated from goniometric measurements, but we could not find a reference to either face in the available literature on corundum crystal morphology.

The habit of the samples grown on spherical seeds is transitional between some natural and some flux-grown—e.g., Knischka (Gübelin, 1982)—crystals. By comparison, the habit of crystals grown on flat seeds is similar to that seen on spherical seeds, but the overall shape of the crystals (e.g., the relative sizes of the different faces) is distorted, because of the different crystallographic orientation and size of the seed plate. Crystals grown on seed plates showed *r*, *n*, and  $\theta$  as major faces, with a smoother surface than their equivalents on crystals with a spherical seed. Minor faces include the hexagonal prism *a* and scalenohedral faces for which indices have not yet been determined.

**Chemistry.** The electron microprobe analyses (table 1) indicate that the chemical composition of the nickel- and chromium-doped hydrothermal synthetic sapphires was about 99.4–99.9 wt.%  $\text{Al}_2\text{O}_3$ . Special attention was paid to measuring the possible chromophores Cr, Ni, Ti, manganese (Mn), and Fe. (Ti, Mn, and Fe are the components of autoclave steel, so they could have entered the growing sapphire through the possible unsealing of the ampoule during the run.) All of the samples including the colorless synthetic sapphire (sample 11; table 1), contain traces of Ti, Mn, and Fe. Since these elements were present in the colorless sample, they apparently do not affect the color at the concentrations present in the Taurus synthetic sapphires.

**Optical Absorption Spectra and Color.** *Optical Absorption Spectra.* Ni-doped sapphire crystals grown by the Verneuil method are known to contain trivalent nickel ( $\text{Ni}^{3+}$ ). To convert the Ni to a divalent state ( $\text{Ni}^{2+}$ ), synthetic sapphire has been annealed in a reducing (hydrogen) atmosphere (Muller and Gunthard, 1966). Minomura and Drickamer (1961) produced  $\text{Ni}^{2+}$ - and  $\text{Ni}^{3+}$ -doped sapphire by annealing pure  $\text{Al}_2\text{O}_3$  crystals in NiO powder. For the samples in our study, however, the  $\text{Ni}^{2+}:\text{Ni}^{3+}$  ratio was set *in situ* during the growth process by controlling the oxidation-reduction potential (see Growth Techniques section), and it varied widely.

The absorption spectrum (in unpolarized light) of  $\text{Ni}^{2+}$ -doped greenish blue Taurus synthetic sapphire (sample 1, table 1) includes three intense bands—at 377, 599, and 970 nm—and two weak bands, at 435 and 556 nm. In polarized light (figure 5A), each intense band is resolved into two bands—that is, 370 and 385 nm, 598 and 613 nm, and 950 and 990 nm (The last two bands are not shown in figure 5A but were detected with the SF-20 spectrophotometer.) These results differ somewhat from the positions reported earlier for  $\text{Ni}^{2+}$  absorption bands in synthetic sapphires grown by other methods (Minomura and Drickamer, 1961; Muller and Gunthard, 1966), which in turn differ noticeably from one another. In particular, lines at 995 and 1020 nm were observed by Minomura and Drickamer, but not by Muller and Gunthard. These differences are understandable given the radically different methods of sapphire growth.

Green synthetic sapphire (sample 9, table 1) grows under relatively high oxidizing conditions, so a greater ratio of  $\text{Ni}^{3+}$  to  $\text{Ni}^{2+}$  is to be expected in a

green crystal. The absorption spectrum of this sapphire (figure 5B) is similar to a  $\text{Ni}^{2+}$  absorption spectrum, but with intense absorption between 380 and 420 nm, rapidly increasing toward the ultraviolet.

The spectra in figure 5C were derived by subtracting the spectra in figure 5A from those in figure 5B: They correlate well with the reported  $\text{Ni}^{3+}$  ion absorption spectrum (Muller and Gunthard, 1966; Boksha et al., 1970). Thus, we believe that the green color of the hydrothermal synthetic sapphires is caused by the simultaneous absorption of  $\text{Ni}^{2+}$  and  $\text{Ni}^{3+}$  ions. As will be shown below, the absorption characterized by the spectrum in figure 5C will produce a yellow color in sapphire. In practice, we have found that by increasing the oxidation potential from a  $\text{Cu}_2\text{O-CuO}$  to a  $\text{PbO-Pb}_3\text{O}_4$  buffer, we can grow yellow sapphire (sample 7, table 1) with a spectrum similar to those in figure 5C.

Another way to produce yellow sapphire doped with  $\text{Ni}^{3+}$  is by gamma irradiation of  $\text{Ni}^{2+}$ -doped pale greenish blue sapphire. The absorption spectra of one of the samples that was gamma-irradiated with 0.5 Mrad (sample 8 in table 1) also resemble those in figure 5C. Moreover, following irradiation, only a weak decrease in  $\text{Ni}^{2+}$  absorption is observed, whereas  $\text{Ni}^{3+}$  absorption increases to become comparable to  $\text{Ni}^{2+}$  absorption.

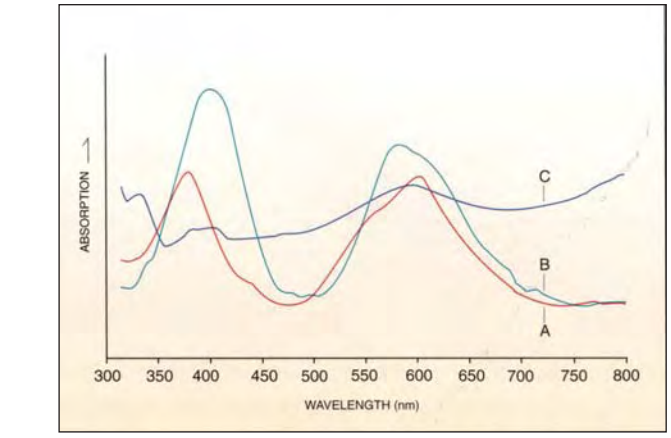
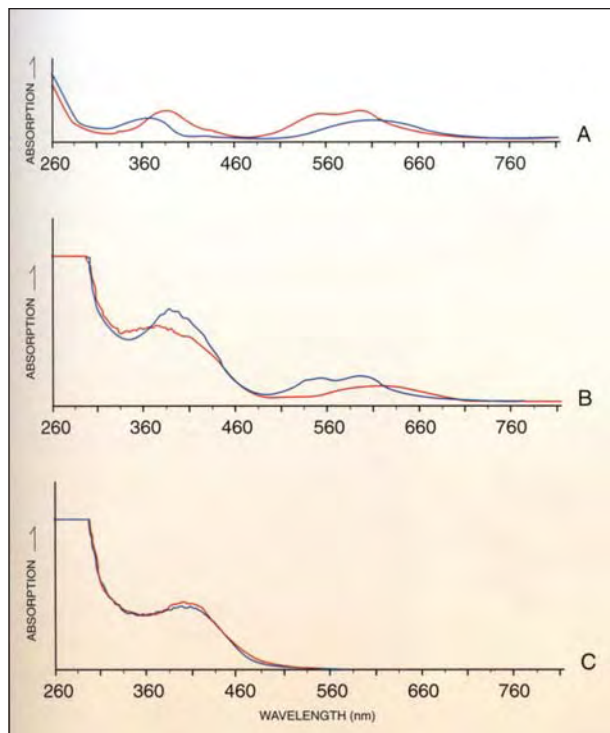


Figure 6. The unpolarized absorption spectra of (A)  $\text{Ni}^{2+}$ -doped and (B)  $\text{Ni}^{2+}$ - $\text{Cr}^{3+}$ -doped Tairus greenish blue synthetic sapphires are quite different from the absorption spectrum of ordinary blue Verneuil-grown  $\text{Fe}^{2+} + \text{Ti}^{4+}$  synthetic sapphire (C). Spectrum C is similar to that of natural  $\text{Fe}^{2+} + \text{Ti}^{4+}$  sapphires.

The addition of small amounts of Cr (up to 0.3 wt.%  $\text{Cr}_2\text{O}_3$ ) to Ni-containing sapphires ( $\text{NiO} > 0.2$  wt.%) results in a greenish blue color, and the simple superposition of Ni and Cr spectra (figure 6). The spectrum of a greenish blue  $\text{Ni}^{2+}$ - $\text{Cr}^{3+}$ -doped sapphire is similar to that of ruby, with characteristic Cr lines at 469, 475 nm, and 690 nm. The band at 510 to 620 nm is a result of the superposition of Ni (580–620 nm) and Cr (510–620 nm) bands. Since this feature is clearly seen in a gemological spectroscope, it can be regarded as a good identifying feature of Tairus greenish blue Cr-containing sapphires.

**Color Varieties.** There are two ways to study and describe color. The first is the “comparison” method, whereby the color of the sample is simply compared to a standard with known color. This method is used in most gemological investigations and for gemological testing. The second way is to calculate color characteristics from the absorption spectra of the gemstones. This method allows us not only to describe the color of these synthetic sap-

Figure 5. These optical absorption spectra are of (A) greenish blue (sample 1, table 1) and (B) green (sample 9, table 1) Tairus synthetic sapphires doped with  $\text{Ni}^{2+}$  and  $\text{Ni}^{2+}$ - $\text{Ni}^{3+}$ , respectively. Spectrum C was produced by subtracting spectrum A from spectrum B and represents a hypothetical yellow synthetic sapphire doped only with  $\text{Ni}^{3+}$ . Blue = parallel to the c-axis; red = perpendicular to the c-axis.

phires, but also to compare them quantitatively to natural sapphires and other synthetics. To quantify the different colors of Tairus hydrothermal synthetic sapphires, we converted their absorption spectra to color coordinates in the CIE color system. The CIE system is fully described elsewhere (Wright, 1964), but a brief explanation of the chromaticity diagram, which is integral to this system, will be made here.

A set of coordinates was developed to express the relationship among all colors in the spectrum on the basis of a "standard observer" response (the average of observations by a large number of people) to different color stimuli. The chromatic portions of these measurements were plotted on an x-y coordinate graph to produce the chromaticity diagram (figure 7). The skewed parabolic curve on this diagram is the location of saturated hue coordinates. The points representing saturated blue and violet colors are located in the left corner of the region, while points of saturated red and orange are on the right. The curved top corresponds to green and yellow saturated colors. The area along the straight line between the violet and red corners is the location of nonspectral purple colors. The point for white color is located in the approximate center of the region; point C marks the white daylight source.

Thus, any hue and saturation can be represented by a set of x-y coordinates and plotted along or within the chromaticity curve. The points shown on the curve are the dominant wavelengths (in nanometers) of each saturated color. Along any radial line drawn between white color and a saturated hue lie colors with decreasing saturation as one approaches the white color point.

The synthetic sapphires doped with  $Ni^{2+}$  (point 1 in figure 7) have a greenish blue hue. The synthetic sapphires grown under oxidizing conditions and colored predominantly by  $Ni^{3+}$  (point 7) are yellow. The position of this point is close to hypothetical  $Ni^{3+}$  sapphire (point 12), which is calculated from the spectra in figure 5C, as well as greenish yellow sapphire (point 8) produced by gamma irradiation. Variations in the ratio of  $Ni^{2+}$  to  $Ni^{3+}$  can produce all of the colors in the region bounded by points 1, 8, 9, and 10.

When significant concentrations of  $Ni^{2+}$  (more than 0.2 wt.% oxide) are present, Cr content has very little impact on the hue of the greenish blue synthetic sapphires. The saturation is slightly lowered (points 2 and 3) and the tone is darkened in the relatively Cr rich samples. When both  $NiO$  and  $Cr_2O_3$  are present at concentrations below 0.1 wt.% each, a light reddish purple (e.g., points 4 and 5) is

Figure 7. On this CIE chromaticity diagram, points are plotted for the Tairus synthetic sapphires (diamond shapes) and for natural and other synthetic sapphires (circles). Points 1 through 10 correspond to the Tairus sample numbers from table 1. Sample 11 is a hydrothermally grown ruby; sample 12 (pure  $Ni^{3+}$ ) was calculated from the spectrum for hypothetical yellow sapphire in figure 5C; and sample 13 is a flame-fusion synthetic ruby. Points 14 through 18 were calculated from representative spectra of natural sapphires by Platonov et al. (1984): 14 is a yellow sapphire from the Ural Mountains, Russia; 15 is a greenish blue sapphire from Australia; 16 is a pale greenish blue sapphire from the Ural Mountains; 17 is a deep blue sapphire that is also from the Urals; and 18 is a deep blue sapphire from Burma. Point "C" represents a standard daylight source. The triangular region defined by the dotted lines illustrates the approximate range of colors produced in Tairus synthetic sapphires by various amounts of  $Ni^{2+}$ ,  $Ni^{3+}$ , and Cr. Note the overlap in color between the Tairus synthetic sapphires and the natural and other synthetic samples.

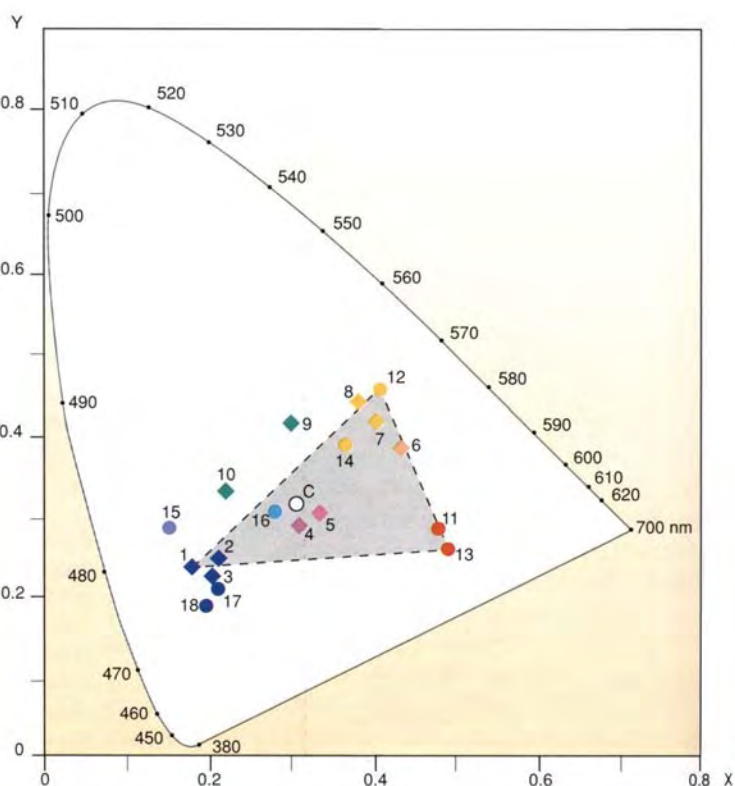


**TABLE 2.** Properties of Tairus greenish blue (Ni<sup>2+</sup> and Ni<sup>2+</sup>-Cr<sup>3+</sup>) synthetic sapphires and some of their natural and other synthetic counterparts.

Property	Tairus hydrothermal synthetic	Chatham Flux-grown synthetic	Flame-fusion synthetic	Natural, from Vietnam	Natural, from Australia	Natural, from China	Natural, from Sri Lanka
Color	Moderately strong, medium to dark greenish blue	Blue	Medium-dark violetish blue (diffusion treated)	Predominantly blue to greenish blue to bluish green, medium-light to very dark	Very slightly greenish blue to greenish blue, and near-colorless to extremely dark "royal" blue	Dark blue with areas bluish green	"Fine" blue of blue and
Color distribution (eye-visible)	Even	Uneven; strong color zoning	Uneven; tiny curved color banding	Uneven; distinct color banding (colorless/blue)	Uneven; color banding (colorless or pale yellow/blue)	Uneven; very strong color zoning	Uneven; very strong color zoning
Pleochroism	Weak (Ni <sup>2+</sup> -Cr <sup>3+</sup> ) to strong green blue to blue (Ni <sup>2+</sup> ); in some cases (Ni <sup>2+</sup> -Cr <sup>3+</sup> ), none	Strong; violetish blue to greenish blue	Strong; violetish blue to grayish blue	Distinct to strong; blue or violetish blue to blue-green or yellow-green	Not reported	Strong	Moderate greenish blue to inky blue
R.I. (n <sub>o</sub> )	1.768–1.769	1.770	1.768	1.769–1.772	1.769–1.772	1.769–1.771	1.768
R.I. (n <sub>e</sub> )	1.759–1.761	1.762	1.759	1.760–1.764	1.761–1.763	1.761–1.762	1.760
Birefringence	0.007–0.010	0.008	0.009	0.008–0.009	0.008–0.009	0.008–0.009	0.008
S.G.	3.98–4.03	3.974–4.035	Not determined	3.99–4.02	3.99–4.02	3.99–4.02	4.00
Fluorescence to LWUV	Typically inert, but in some cases (with high Cr) purplish red	Variable, inert to strong in yellow to orange	Inert	Inert	Inert	Inert	Inert
Fluorescence to SWUV	Typically inert, but in some cases (with high Cr) very weak purplish red	Variable, inert to strong in green, yellow to orange colors	Chalky light blue	Inert	Inert	Inert	Light blue
Reference	Present study	Kane (1982)	SGC Databank <sup>a</sup>	Smith et al. (1995)	Coldham (1985)	Furui (1988)	Gunawardene and Rupasinghe (1986)

<sup>a</sup>Stones tested in the Siberian Gemological Center (SGC).

produced. The addition of small amounts of Cr<sup>3+</sup> to Ni<sup>3+</sup>-doped synthetic sapphire shifts the hue from yellow (such as for point 7) to the orange part of the spectrum, producing a "padparadscha" type pinkish orange color (point 6). Thus, addition of Cr to either Ni<sup>2+</sup> or Ni<sup>3+</sup> shifts the color coordinates toward purple, near the lines connecting point 13 with points 1 and 12.

The combination of different amounts of Cr<sup>3+</sup>, Ni<sup>2+</sup>, and Ni<sup>3+</sup> permits the production of synthetic sapphires in virtually any color in the vicinity of triangle 1-12-13 (shaded triangle on figure 7). The hue and saturation are strongly dependent on the concentrations of these elements. Thus, although the triangle 1-12-13 does not represent absolute boundaries (e.g., points 3, 9, and 10 do lie away from the

triangle), it helps to illustrate the range of colors represented by the samples grown in our experiments and discussed in this article. In addition, figure 7 shows that the colors of some Tairus synthetic sapphires overlap the colors of their natural counterparts, as well as the colors of synthetic sapphires grown by other methods.

**Gemological Characteristics.** The properties for greenish blue, pinkish orange (padparadscha), and yellow Tairus hydrothermal synthetic sapphires are reported in tables 2, 3, and 4, respectively. Sample stones are illustrated in figures 8, 9, and 10, respectively. The blue and pinkish orange samples are compared to Chatham flux-grown synthetic sapphires and flame-fusion samples from an unknown

**TABLE 3.** Properties of Tairus pinkish orange “padparadscha” (Ni<sup>3+</sup>-Cr<sup>3+</sup>) synthetic sapphires and some of their natural and other synthetic counterparts.

Property	Tairus hydrothermal synthetic	Chatham Flux-grown synthetic	Flame-fusion synthetic	Natural, from Sri Lanka
Color	Medium-light moderate pinkish orange	Orange to reddish orange, in moderate to vivid saturation	Orange to yellowish orange, in medium-light to medium-dark tones, moderate to strong saturation	Pinkish orange <sup>a</sup>
Color distribution (eye-visible)	Even	Color zoned	Even	Not reported
Pleochroism	Weak reddish orange and light reddish orange	Strong pink and orange to brownish yellow	Weak to moderate orangy yellow and yellowish-orange	Orange-yellow and yellowish orange
R.I. (n <sub>ω</sub> )	1.765	1.770	1.768	1.768
R.I. (n <sub>ε</sub> )	1.757	1.762	1.759	1.760
Birefringence	0.008	0.008	0.009	0.008
S.G.	4.00	4.00 ± 0.003	3.97	4.00
Fluorescence to LWUV	Moderate orange	Strong to very strong orange-red to yellowish orange	Weak orange-red	Strong “apricot” <sup>b</sup>
Fluorescence to SWUV	Weak orange	Very weak to weak in same colors as LW	Inert	Strong “apricot” <sup>b</sup>
Reference	Present study	Kane (1982)	SGC Databank <sup>c</sup>	Gunawardene and Rupasinghe (1986)

<sup>a</sup>Crowningshield (1983).

<sup>b</sup>Type of UV radiation was not specified.

<sup>c</sup>Stones tested in the Siberian Gemological Center (SGC).

manufacturer; all three hue types are compared to natural sapphires from various sources worldwide.

The refractive indices of the Tairus synthetic greenish blue samples were found to be near the lower limits of corundum (see, e.g., Feklichev, 1989). As shown in table 2, they overlap the R.I. values reported for Sri Lankan sapphires and flame-fusion synthetic sapphires, and they are slightly below the values reported for the flux-grown synthetic sapphires and natural sapphires from the other sources. The values obtained for the yellow and pinkish orange Tairus synthetic sapphires were somewhat lower still. Some of the pinkish orange Tairus samples had values below the known range for corundum (see, e.g., Feklichev, 1989). The pink (n<sub>ω</sub>=1.765, n<sub>ε</sub>=1.758) and dark green (n<sub>ω</sub>=1.768, n<sub>ε</sub>=1.760) samples—not reported in the tables—showed values that were between those of the yellow-to-orange (including padparadscha) and greenish blue samples. The refractive indices of the pink samples were close to those reported for Chatham flux-grown synthetic pink sapphires (n<sub>ω</sub>=1.768, n<sub>ε</sub>=1.759; Kammerling et al., 1994), and they fell within the ranges reported for

other hydrothermal lab-grown sapphires. As indicated in tables 2–4, the values for birefringence and specific gravity of the Tairus hydrothermal synthetic sapphires overlap those for these natural and other synthetic sapphires.

**Dichroism.** Ni<sup>2+</sup>-doped synthetic sapphires (e.g., sample 1 in table 1) showed a strong green-blue to blue dichroism. In the blue-green Ni<sup>2+</sup>-Ni<sup>3+</sup>-doped samples (e.g., sample 10), dichroism was strong violetish blue to blue-green; in the green (e.g., sample 9) Ni<sup>2+</sup>-Ni<sup>3+</sup>-doped samples, the colors were somewhat weaker brownish green and green. Increasing Cr content in the greenish blue Ni<sup>2+</sup>-Cr<sup>3+</sup>-doped synthetic sapphires weakens their dichroism. In greenish blue Cr-rich sapphires (e.g., sample 3), dichroism was clearly visible only with a bright incandescent light source: A light purple tint was seen in one direction. This purple tint is due to chromium’s characteristic red luminescence to incandescent light. Even with an ordinary incandescent lamp, purple flashes can be seen in faceted samples viewed face-up. These features of greenish blue Cr-rich Tairus synthetic sap-



Figure 8. Tairus researchers produced these greenish blue hydrothermal synthetic sapphires by doping them with  $\text{Ni}^{2+}$  and  $\text{Ni}^{3+}$  and, in some cases,  $\text{Cr}^{3+}$ . Photo © GIA and Tino Hammid.

phires can help to distinguish them from their natural and other synthetic counterparts. The yellow sapphires colored predominantly by  $\text{Ni}^{3+}$  showed no dichroism, whereas the addition of Cr to  $\text{Ni}^{3+}$  resulted in weak dichroism in the pinkish orange (padparadscha) sapphires.

**Reaction to Ultraviolet Radiation.** Sapphire's luminescence to UV radiation strongly depends on Cr content. The greenish blue Cr-rich synthetic sapphires in this study fluoresced red to both short-wave (SW) and long-wave (LW) ultraviolet, whereas the greenish blue Ni-rich samples were inert to both. The fluorescence of the greenish blue Cr-rich samples was much weaker to SWUV than to LWUV. Red fluorescence has not been observed in most natural (except some light blue Sri Lankan and some rare dark blue stones [*Gem Reference Guide*, 1995]) or other synthetic blue sapphires, so it can be used as a diagnostic feature for greenish blue Cr-rich Tairus synthetic sapphires.

"Padparadscha"-colored samples fluoresced moderate orange to LWUV and weak orange to SWUV—reactions different from those of the natural and other synthetic sapphires of similar color reported in table 3. However, the reaction of natural yellow sapphires to UV radiation varies considerably, so this feature cannot serve to separate Tairus synthetic sapphires from natural stones of this color.

**Inclusions and Other Internal Features.** Some of the samples studied were internally flawless; others contained various amounts of inclusions. These internal features consisted of fluid inclusions, crystalline inclusions, and optical inhomogeneities.



Figure 9. The colors of these pinkish orange "padparadscha" ( $\text{Ni}^{3+}$ - $\text{Cr}^{3+}$ ) Tairus hydrothermal synthetic sapphires are similar to those seen in nature or in other synthetic sapphires. Photo © GIA and Tino Hammid.

Figure 10. Yellow Tairus hydrothermal synthetic sapphires are colored predominantly by  $\text{Ni}^{3+}$ . Photo © GIA and Tino Hammid.



**TABLE 4.** Properties of Tairus yellow ( $\text{Ni}^{3+}$ - $\text{Ni}^{2+}$ ) synthetic sapphires and some of their natural and other synthetic counterparts.

Property	Tairus hydrothermal synthetic	Natural, from Australia	Natural, from Sri Lanka
Color	Yellow to greenish yellow, light tones, strong saturation	Light yellow to strong "golden" yellow	Intense "golden" yellow to light or pale yellow
Color distribution (eye-visible)	Even	Occasionally color zoned	Not reported
Pleochroism	None	Not reported	Orangy yellow to grayish yellow
R.I. ( $n_o$ )	1.767–1.765	1.774–1.772	1.768
R.I. ( $n_e$ )	1.758	1.765–1.763	1.760
Birefringence	0.007–0.009	0.008–0.009	0.008
S.G.	3.98	3.97–4.01	4.02
Fluorescence to LWUV	Inert or weak orange	Inert	"Apricot" red
Fluorescence to SWUV	Inert or very weak orange	Inert	"Apricot" orange
Reference	Present study	Coldham (1985)	Gunawardene and Rupasinghe (1986)

*Two- and Three-Phase (Primarily Liquid) Inclusions.* These could be divided into two major types. In both types, the inclusions consisted of two (gas-liquid) or three (a liquid, a gas, and a small crystal) phases. Two-phase inclusions were much more common than three-phase ones. Crystal phases were uncommon, but those present were easily seen in polarized light.

The first type consists of large inclusions with an irregular, elongate form located along planes perpendicular to the seed and running along planes parallel to one pair of the prismatic *a* faces (figure 11). We believe that these are primary (see, e.g., Roedder, 1984), formed when a small portion of growth solution was trapped under a crystal face during growth. These inclusions were apparently captured in flattened depressions on the surface of the growing crystal. Such depressions are typical of hydrothermal crystals grown on a seed (Smirnov, 1997). They were observed in only two faceted stones and a few crystals, which were blue, yellow, and colorless.

The second type are typical "fingerprints" (figure 12), with regular to irregular patterns confined to healed fractures, and therefore are secondary (see, e.g., Roedder, 1984). They also form perpendicular to the seed plate and extend in both directions. "Finger-

prints" were found in many faceted stones and in most of the crystals, in samples of almost all colors.

*Crystalline Inclusions.* Almost all of the green-to-blue samples examined contained crystalline inclusions. In some cases, these were single crystals that could be resolved only with high magnification and immersion. Other samples contained abundant inclusions in the form of small, flake-like aggregates of tiny crystals (figure 13); these inclusions could be clearly seen with a hand loupe. In some cases, when examined with bright, fiber-optic, oblique illumination, most of these crystalline inclusions appeared to have a metallic luster. With high magnification, they appeared to be opaque isometric grains a few micrometers in diameter. Because the growth process used Cu-containing oxygen buffers, it is likely that this metallic phase is copper.

Other crystals in these aggregates were transparent, colorless or near-colorless, and isotropic with an octahedral shape (figure 14). Because the individual crystals were so small (less than about 12  $\mu\text{m}$ ), we could not determine their composition with the available instrumentation. However, our recent experiments have revealed that the addition of a small amount of Mg to an alumina-bearing solution leads to the formation of spinel ( $\text{MgAl}_2\text{O}_4$ ) crystals. Trace amounts of Mg could occur as an impurity in the charge used for the autoclave, so we suggest that these octahedra are spinel crystals.

Another type of transparent crystal was seen in the green synthetic sapphires. These crystals appeared as isolated platelets with regular hexagonal outlines and no apparent color (figure 15). The optical properties of these crystals suggest that they are gibbsite.

*Optical Inhomogeneities and Color Zoning.* We observed characteristic optical inhomogeneities—swirl- and chevron-like patterns—in all the greenish blue and green specimens, rough as well as faceted (figure 16). These terms commonly refer to wavy or angular features inside synthetic or natural crystals.

The swirl-like patterns resemble textures that can be seen in artificial glass. When the faceted samples were examined face up, these patterns appeared as very faint, contrasting wavy lines. Chevron patterns were seen in the same samples, but at an angle to the table plane. These swirls and chevrons were much more visible in the darker samples than in the lighter ones. They were less distinct in the pinkish orange (padparadscha type) syn-

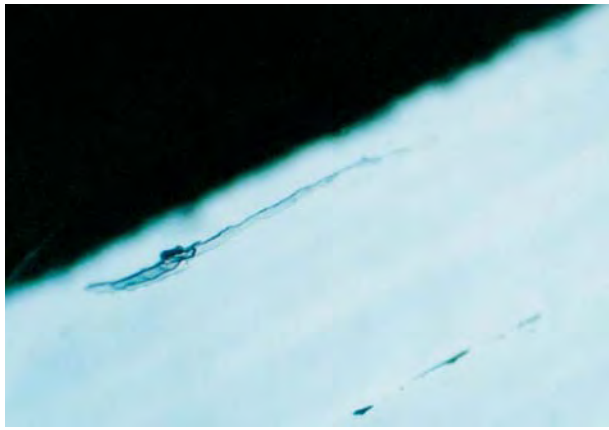


Figure 11. Irregular, elongate fluid-and-gas inclusions were found in some blue, yellow, and colorless Tairus synthetic sapphires, located along crystallographically oriented planes. Photomicrograph by S. Z. Smirnov; magnified 100 $\times$ .

thetic sapphires and were not observed at all in the yellow or light pink samples.

Our studies revealed that the swirls and chevrons were typically seen in those samples that were grown on a seed plate with planar surfaces cut so as to be oriented at an angle to actual crystal faces (i.e., on a nonsingular crystal surface). They were found to represent boundaries between growth sectors of subgrains that formed on the seed plate as the crystal grew. Thus, the appearance of these patterns will be affected by the orientation of the table of a faceted stone. They are distinctly different from the angular growth zones found in natural and in flux-grown synthetic sapphires. Nor do they resemble the curved growth zoning usually seen in Verneuil-grown synthetic sapphires.

In several cross-sections of greenish blue Tairus

Figure 12. "Fingerprints" are common in the Cr- and Ni-doped Tairus synthetic sapphires. Photomicrograph by S. Z. Smirnov; magnified 100 $\times$ .

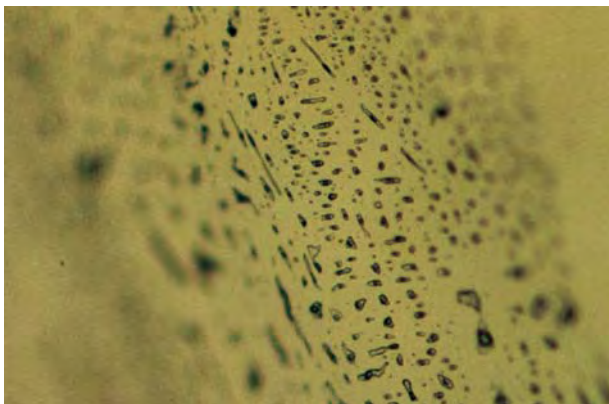


Figure 13. Flake-like crystalline inclusions are abundant in many of the green-to-blue Tairus hydrothermal synthetic sapphires. Photomicrograph taken by S. Z. Smirnov, with sample between crossed polarizers, immersed in methylene iodide, magnified 25 $\times$ .

samples, we observed color zoning parallel to the plane of the seed plate. The portion of the crystal nearest the seed plate was yellow, while the rest was greenish blue. This thin (about 0.5 mm) sharp zone is usually cut away during pre-forming, so it is seen only rarely in faceted stones.

**Infrared Spectroscopy.** Hydrothermally grown crystals commonly contain water in different forms. This is also true for corundum, both natural (see Smith, 1995, and references therein) and hydrothermal synthetic stones (Peretti and Smith, 1993). In rare cases, traces of water as OH<sup>-</sup> groups may be found in Verneuil-grown crystals (Volynets et al., 1974; Beran, 1991). The form of water incorporation into sapphire and ruby has been the focus of many studies, because it can help clarify the genesis of the gem. Today it is generally accepted, on the basis of infrared spectroscopy, that water as OH<sup>-</sup> groups enters the corundum structure as a compensating charge due to either the doping of the corundum with divalent cations or the formation of Al vacancies in the structure (Muller and Gunthard, 1966; Volynets et al., 1974; Beran, 1991). To examine this issue and also further distinguish the Tairus synthetic sapphires from their natural and other synthetic counterparts, we conducted an IR-spectroscopic study of the Tairus Ni- and Cr-doped hydrothermal synthetic sapphires.

The IR spectra of the greenish blue and green synthetic sapphires (samples 1 and 9, respectively, in table 1) are similar in the 4000-1600 cm<sup>-1</sup> region (figure 17). This region is characterized by an intense wide band, with a maximum at 2980 cm<sup>-1</sup>; a narrow peak at 2750 cm<sup>-1</sup>; and five narrow peaks in

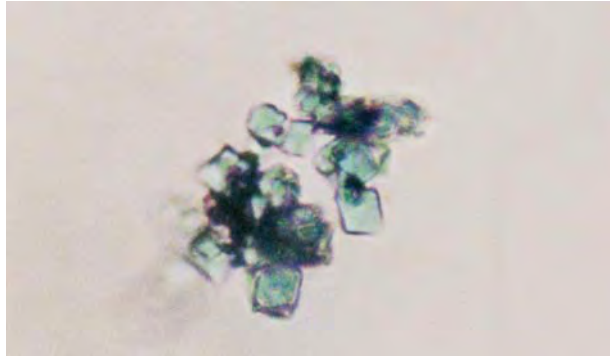


Figure 14. At high (500 $\times$ ) magnification, small transparent octahedral crystals (possibly spinel) can be seen inside some of the aggregates in greenish blue sapphires shown in figure 13. Photomicrograph by S. Z. Smirnov.

the region between 2500 and 2000  $\text{cm}^{-1}$ . In the spectrum of the greenish blue sapphire (A), there is a shoulder near 3300  $\text{cm}^{-1}$ . In the spectrum for the green sample (B), two narrow peaks are superimposed on the wide band at 3400 and 3310  $\text{cm}^{-1}$ .

The presence of an intense wide band near 3000  $\text{cm}^{-1}$  is attributed to  $\text{OH}^-$  groups contained in aluminum oxides. It is observed in the IR spectra of diaspore ( $\text{AlOOH}$ ; Ryskin, 1974) and in the spectra of natural corundum containing divalent cations (Muller and Gunthard, 1966; Eigenmann and Gunthard, 1971; Volynets et al., 1974). The IR spectra of the Tairus Ni-doped synthetic sapphires (see figure 17) are similar to those for Ni-containing corundum grown by the Verneuil method in a reducing, hydrogen atmosphere (Eigenmann and Gunthard, 1971). Following these authors, we believe that the 2980  $\text{cm}^{-1}$  band is the absorption band of  $\text{OH}^-$  groups that compensate the charge for the  $\text{Al}^{3+} + \text{O}^{2-} \rightarrow \text{Ni}^{2+} + (\text{OH})^-$  replacement.

The narrow peaks observed between 3600 and 3000  $\text{cm}^{-1}$  are also related to the absorption of  $\text{OH}^-$  groups which compensate for charge deficiency due to the formation of cation vacancies. These peaks have been reported both for natural (Smith, 1995, and references therein) and synthetic corundum (Belt, 1967; Eigenmann and Gunthard, 1971; Volynets, 1974; Beran, 1991; Peretti and Smith, 1993, 1994). The peaks at 3310 and 3400  $\text{cm}^{-1}$ , observed in the infrared spectrum of our green sample (see figure 17), were also reported earlier (Smith, 1995).

Peaks near 2000  $\text{cm}^{-1}$  may be observed in the IR spectra of other  $\text{OH}^-$  containing aluminum oxides. However, the peaks at 2114 and 1984  $\text{cm}^{-1}$  that are present in the spectrum of diaspore (Ryskin, 1974; Smith, 1995) were absent from the spectra of our hydrothermal synthetic sapphires. Therefore, we



Figure 15. In the green hydrothermal synthetic sapphires, the transparent crystals appeared to be anisotropic hexagonal platelets, which may be gibbsite. When viewed between crossed polarizers, they showed a bright interference color. Photomicrograph by S. Z. Smirnov; magnified 500 $\times$ .

believe that the bands near 2000  $\text{cm}^{-1}$  in our samples are not related to diaspore inclusions, especially as the samples studied were free of inclusions (at 100 $\times$  magnification). The IR absorption lines for  $\text{CO}$  molecules may occur between 2133 and 2148  $\text{cm}^{-1}$  (Hallam, 1973). Wood and Nassau (1967) observed the absorption bands related to  $\text{CO}_2$  molecules in beryl structure channels at 2354  $\text{cm}^{-1}$ . Because the Tairus crystals grew in carbonate solutions of complex composition, the incorporation of  $\text{CO}$ ,  $\text{CO}_2$ ,  $\text{CO}_3^{2-}$ , and other forms of carbon oxides into the growing crystal is very likely. Thus, we believe that the narrow bands at 2460, 2400, 2264, 2136, and

Figure 16. Swirl-like and chevron patterns were commonly seen in the Tairus synthetic green-to-greenish blue sapphires. Immersed in methylene iodide, magnified 100 $\times$ ; photomicrograph by S. Z. Smirnov.



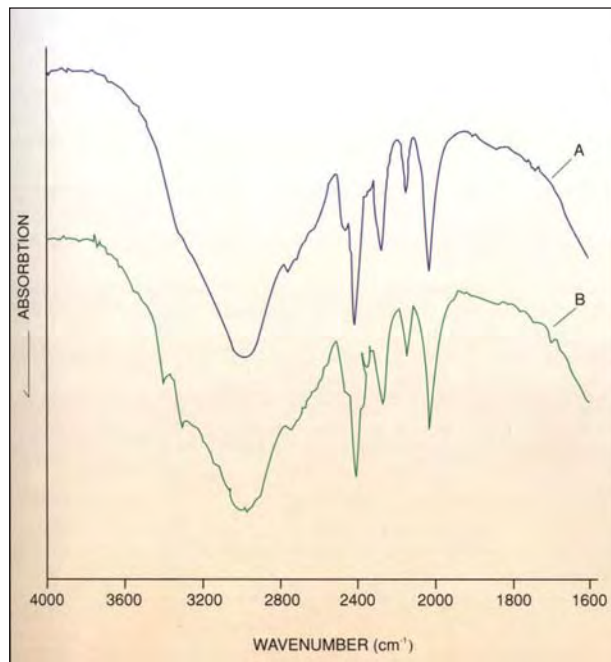
2016  $\text{cm}^{-1}$  could be related to the C–O bond in different carbon oxides that were incorporated into the sapphire crystals. Strong pleochroism is another feature of these bands, which suggests that these C–O bonds are part of the corundum structure and are not caused by separate carbon oxide species (e.g., CO or  $\text{CO}_2$  in fluid inclusions).

These bands were also reported for Tairus hydrothermal synthetic rubies by Peretti and Smith. (1993). We have not found a description of such bands in the literature for natural and other synthetic sapphires. Therefore, we believe that the five narrow peaks between 2500 and 2000  $\text{cm}^{-1}$  are characteristic of Tairus synthetic sapphires.

### IDENTIFYING CHARACTERISTICS OF TAIRUS HYDROTHERMAL SYNTHETIC SAPPHIRES

Previously, blue, green, and yellow sapphires were grown only by flux- or melt-growth techniques, but the synthetic sapphires studied for this article more closely resemble their natural counterparts because they have been grown from a hydrothermal solution, as takes place frequently in nature. Nevertheless, there are a number of features by which an

Figure 17. The infrared absorption spectra of greenish blue (A) and green (B) Tairus synthetic sapphires are very similar (they are shown here offset for purposes of comparison). The curves have been corrected for a spurious absorption attributed to  $\text{CO}_2$ .



experienced gemologist can separate these sapphires from their natural counterparts and other synthetic sapphires:

1. The swirl-like patterns observed in Tairus synthetic sapphires are common to most synthetic crystals grown on seed plates under hydrothermal conditions and are rare for natural stones.
2. The red reaction to UV radiation of the greenish blue synthetic sapphires containing Cr is different from that of most natural and other synthetic sapphires.
3. The crystalline copper inclusions and flake-like aggregates seen in the Tairus synthetics are not present in natural sapphires. Metallic inclusions are common in melt- and flux-grown synthetics, but they usually consist of platinum-group metals.
4. Ni, an important chromophore in the Tairus synthetic sapphires, is not found in natural sapphires or most synthetic ones.
5. The absorption spectra of the greenish blue Ni-doped Tairus synthetic sapphires differ from those of natural blue sapphires, which owe their color to Fe and Ti. The spectrum (in unpolarized light) of a greenish blue Tairus synthetic sapphire includes three intense bands—at 377, 599, and 970 nm—and two weak bands, at 435 and 556 nm.
6. Five narrow peaks between 2500 and 2000  $\text{cm}^{-1}$  in the infrared spectra of Tairus synthetic sapphires clearly separate them from their natural and other synthetic counterparts.

### CONCLUSION

The technology to manufacture synthetic sapphire in a wide variety of colors by means of hydrothermal growth has been developed by researchers of the Tairus joint venture. This was achieved by doping synthetic corundum with different amounts of  $\text{Ni}^{2+}$ ,  $\text{Ni}^{3+}$  and  $\text{Cr}^{3+}$ . Specific colors are also produced by controlling the oxidation-reduction environment. Although these colors overlap those of most natural and other synthetic sapphires, the Tairus synthetic sapphires can be readily identified on the basis of their distinctive internal features (swirl-like patterns and copper inclusions), visible-range and infrared spectra, and the presence of Ni as a trace element.

To date, thousands of hydrothermal synthetic sapphires have been grown at the Tairus factory in

Novosibirsk (Russia) and cut at the Pinky Trading Co. facilities in Bangkok. Greenish blue, pinkish orange, and yellow sapphires are commercially available as cut stones up to 4 ct.

*Acknowledgments: The authors are grateful to Ivan Foursenko and Alexander Dokukin for the samples of hydrothermal synthetic ruby donated for this study. Special thanks to Evgeny Krayushin for the photos of synthetic sapphires studied. This work has benefited from discussions with Dr. Dmitry Foursenko, Taurus director of research, and Dr. Vladislav Shatsky, director of the Siberian Gemological Center.*

## REFERENCES

- Belt R.F. (1967) Hydrothermal ruby: infrared spectra and X-ray topography. *Journal of Applied Physics*, Vol. 38, No. 6, pp. 2688–2689.
- Beran A. (1991) Trace hydrogen in Verneuil-grown corundum and its color varieties: an IR spectroscopic study. *European Journal of Mineralogy*, Vol. 3, No. 6, pp. 971–975.
- Boksha O.N., Grum-Grzymailo S.V., Pasternak L.B., Popova A.A., Smirnova E.F. (1970) Synthesis and optical spectra of corundums doped with transition elements. In S.V. Grum-Grzymailo, B.S. Skorobogatov, P.P. Feofilov, and V.I. Cherepanov, Eds., *Spectroscopy of Crystals*, "Nedra," Moscow, pp. 295–302 (in Russian).
- Burns R.G. (1981) Intervalence transition in mixed-valence minerals of iron and titanium. In G.W. Wetherill, A.L. Albee, and F.G. Stehli, Eds., *Annual Review of Earth and Planetary Sciences*, Vol. 9, Annual Reviews Inc., Palo Alto, CA, pp. 345–383.
- Catalogue of Colored Glasses* (1967). "Mashinostroenie," Moscow (in Russian).
- Coldham T. (1985) Sapphires from Australia. *Gems & Gemology*, Vol. 21, No. 3, pp. 130–146.
- Crowningshield R. (1983) Padparadscha: What's in a name? *Gems & Gemology*, Vol. 19, No. 1, pp. 30–36.
- Eigenmann K., Gunthard Hs.H. (1971) Hydrogen incorporation in doped  $\alpha$ -Al<sub>2</sub>O<sub>3</sub> by high temperature redox reactions. *Chemical Physics Letters*, Vol. 12, No. 1, pp. 12–15.
- Feklichev V.G. (1989) *Diagnostic Constants of Minerals*. "Nedra," Leningrad (in Russian).
- Furui W. (1988) The sapphires of Penglai, Hainan Island, China. *Gems & Gemology*, Vol. 24, No. 3, pp. 155–160.
- Gem Reference Guide* (1995) Gemological Institute of America, Santa Monica, CA, 270 pp.
- Goldschmidt V. (1916) *Atlas der Krystalformen*. Carl Winters Universitätsbuchhandlung, Heidelberg.
- Gübelin E. (1982) New synthetic rubies made by Professor P.O. Knischka. *Gems & Gemology*, Vol. 18, No. 3, pp. 165–168.
- Gunawardene M., Rupasinghe S. (1986) The Elahera gem field in central Sri Lanka. *Gems & Gemology*, Vol. 22, No. 2, pp. 80–95.
- Hallam H.E. (1973) Molecules, trapped in low temperature molecular matrices. In Hallam H.E., Ed., *Vibrational Spectroscopy of Trapped Species: Infrared and Raman Studies of Matrix-Isolated Molecules, Radicals and Ions*, Wiley-Interscience, London-New York, pp. 68–132.
- Kammerling R.C., Koivula J.I., Fritsch E. (1994) An examination of Chatham flux-grown synthetic pink sapphires. *Journal of Gemmology*, Vol. 24, No. 3, pp. 149–154.
- Kane R. (1982) The gemological properties of Chatham flux-grown synthetic orange sapphire and synthetic blue sapphire. *Gems & Gemology*, Vol. 18, No. 3, pp. 140–153.
- Kuznetsov V.A., Shternberg A.A. (1967) Crystallization of ruby under hydrothermal conditions. *Soviet Physics-Crystallography*, Vol. 12, No. 2, pp. 280–285.
- Laudise R.A., Ballman A.A. (1958) Hydrothermal synthesis of sapphire. *Journal of the American Chemical Society*, Vol. 80, pp. 2655–2657.
- Minomura S., Drickamer H.G. (1961) Effect of pressure on the spectra of transition metal ions in MgO and Al<sub>2</sub>O<sub>3</sub>. *Journal of Chemical Physics*, Vol. 35, No. 3, pp. 903–907.
- Muller R., Gunthard Hs.H. (1966) Spectroscopic study of the reduction of nickel and cobalt ions in sapphire. *Journal of Chemical Physics*, Vol. 44, No. 1, pp. 365–373.
- Peretti H.A., Smith C.P. (1993) A new type of synthetic ruby on the market: Offered as hydrothermal rubies from Novosibirsk. *Australian Gemmologist*, Vol. 18, No. 5, pp. 149–157.
- Peretti H.A., Smith C.P. (1994) Letters to the editor. *Journal of Gemmology*, Vol. 24, No. 1, pp. 61–63.
- Platonov A.N., Taran M.N., Balitsky V.S. (1984) *The Nature of Gemstone Colors*. "Nedra," Moscow, 196 pp. (in Russian).
- Roedder E. (1984) Fluid inclusions. *Reviews in Mineralogy*, Vol. 12, 644 pp.
- Ryskin Ya.I. (1974) The vibration of protons in minerals: Hydroxyl, water and ammonium. In Farmer V.C., Ed., *The Infrared Spectra of Minerals*, Mineralogy Society Monograph, London, pp. 137–181.
- Smirnov S. (1997) The inclusions of mineral-forming media in synthetic and natural gemstones (formation mechanisms and genetic application). Ph.D. diss., Novosibirsk (in Russian).
- Smith C.P. (1995) A contribution to understanding the infrared spectra of rubies from Mong Hsu, Myanmar. *Journal of Gemmology*, Vol. 24, No. 5, pp. 321–325.
- Smith C.P., Kammerling R.C., Keller A.S., Peretti A., Scarratt K.V., Nguen Dang Khoa, Repetto S. (1995) Sapphires from Southern Vietnam. *Gems & Gemology*, Vol. 31, No. 3, pp. 168–188.
- Volynets F.K., Sidorova E.A., Stsepuro N.A. (1974) OH<sup>-</sup> groups in corundum crystals which were grown with the Verneuil technique. *Journal of Applied Spectroscopy*, Vol. 17, No. 6, pp. 1626–1628.
- Wood D.L., Nassau K. (1967) Infrared spectra of foreign molecules in beryl. *Journal of Chemical Physics*, Vol. 47, No. 7, pp. 2220–2228.
- Wright W.D. (1964) *The Measurement of Colour*, 3<sup>rd</sup> ed. Van Nostrand, New York, 291 pp.
- Yakubova V.V. (1965) Corundum. In F.V. Chukhrov and E.M. Bornshted-Kupletska, Eds., *Minerals*, Nauka, Moscow, pp. 63–75 (in Russian).